Contents lists available at Science-Gate

International Journal of Advanced and Applied Sciences

Journal homepage: http://www.science-gate.com/IJAAS.html

Delineation of reservoir lateral continuity for flow zones in wells using cluster analysis: Case of West Baram Delta, offshore-Sarawak

I. Yusuf [1, 2, *], E. Padmanabhan [1]

[1]Department of Geosciences, Faculty of Geosciences and Petroleum Engineering, Universiti Teknologi PETRONAS, Postcode 32610, Seri Iskandar, Perak, Malaysia
[2]Department of Geology and Mining, Faculty of Applied Science and Technology, IBB University, Lapai Niger State, Nigeria

ARTICLE INFO

Article history:
Received 28 October 2018
Received in revised form
4 February 2019
Accepted 5 February 2019

Keywords:
Petrofacies
Flow zone
Reservoir lateral continuity
Cluster analysis
West Baram Delta

ABSTRACT

Reservoir property modeling is often used to determine lateral extent and continuity in targeted multiple wells for implementation of any enhanced oil recovery (EOR) methods. Some works were reported that most of EOR techniques are controlled by static-dynamic lateral extent and continuity within reservoir pay zones succession as they contribute to poor recovery in fields. Therefore, delineation of lateral extent and continuity using a statistical approach could save time, less cumbersome and data required. This paper by cluster analysis delineates lateral extent of 5 exploratory wells by integration of microscopic petrographic and petrophysical data from 132 subsurface and 97 core plugs. Result reveal four main petrofacies clusters of good lateral extent and continuity that corresponds to section (Blue cluster) characterized by massive coarse grained sandstones, massive fine grained sandstones and massive very fine grained sandstone lithofacies with average porosity (18 - 32%), permeability (400 -1189 mD) at depths between 859 and 2129m. The Green cluster is dominated by massive fine grained and massive medium grained sandstone lithofacies exhibit average porosity (15-30%), permeability (110 - 840 mD) at depth from 880 - 1805m, while Brown cluster comprises of massive medium grained and massive fine grained sandstone lithofacies exhibit an average porosity (18 -25%) and permeability (210-657 mD). The understandings of porosity-permeability continuity can facilitate effective areal sweep efficiency from injected fluid well to production well during recovery. Thus, this approach is important to improve the field plan for reservoir engineers.

1. Introduction

Reservoir lateral extent is crucial for successful implementation of any enhanced oil recovery (EOR) methods for effective areal sweep efficiency between injection and production wells during recovery in the field (Weijermars and van Harmelen, 2017). It described that the spatial and temporal variations in reservoir petrophysical properties (porosity-permeability) distribution has an enormous effect on successful implementation of any EOR methods in the field (Ebanks, 1987). Flow zones are mappable units of reservoirs having consistent geological and petrophysical parameters affecting fluid flow (Ringrose and Bentley, 2015) extent and distribution. These zones are mainly delineated through reservoir property modeling and simulation (Ringrose and Bentley, 2015) approach, but requires large of volume data by introduction of representative elementary volume (REV) (Bear and Bachmat, 2012) to develop dynamic version of geological flow zones. Therefore, it is paramount due to ongoing enhanced oil recovery phase in the West Baram Delta to delineate reservoir lateral extent as one of prerequisite required for effective areal and lateral sweep efficiency in reservoirs. As emphasis to maximize oil recovery from mature fields (Latief et al., 2012) around the world prompt renewed interest (Henares et al., 2014) to understand the distribution of fluid flow characteristic (porosity and permeability) in wells, since it is associated with changes in vertical and horizontal properties that occurred due to difference in depositional environments. These differences affect spatial and temporal distribution in porosity-permeability that determines reservoir extent and continuity between

* Corresponding Author.
Email Address: ishaq.yusuff@gmail.com (I. Yusuf)
https://doi.org/10.21833/ijaas.2019.04.003
Corresponding author's ORCID profile:
https://orcid.org/0000-0002-1534-3052

two or more wells. To a geoscientist, a flow zone is a definable facies object such as a fluvial channel or shallow marine sandbar; to a petrophysicist, it is correlatable zone with similar porosity, permeability and net-to-gross ratio; to a reservoir engineers, it is a layer in the reservoir that has a consistent dynamic response in the simulator; to a reservoir modeler it is all of these things (Ringrose and Bentley, 2015). Statistical exploratory method of data mining (Surek, 2013) places fluid flow characteristic properties into more homogeneous cluster (fluid flow zone) in a manner that relation between similar facies are revealed in their extent and lateral continuity across wells. This article present a more simplify approach to delineate similar flow units using statistical cluster analysis for different reservoir layers at variable depths from core plugs and petrographic data to improve reservoir description (Amaefule et al., 1993) for successful implementation of enhanced oil recovery.

The understanding of gross distribution of fluid flow zones at variable depths and interval drives the internal layering of reservoir zones, would lead to stratigraphic correlation and hierarchy of each reservoir well sections for effective areal sweep efficiency.

2. Geological and stratigraphy setting

The West Baram Delta is one of prolific geological provinces in offshore the Sarawak foreland basin, estimated to have more than 400 million stock barrels of oil in-place with multiple stacked reservoir in the shallow marine offshore environment (Darman et al., 2007) in Fig. 1 (Rahman et al., 2014; Hutchison, 2005). The delta is currently having an average production rate of 30% Bakar (Abu Bakar et al., 2011; Ben-Awuah et al., 2016) in more than 160 exploratory wells. However, increase in emphasis to maximize oil recovery from existing fields (Henares et al., 2014) has prompted renewed interest to review the temporal and spatial distribution of porosity and permeability properties across selected production wells in the area. More so, literature reveals that there are substantial heterogeneity within approximately 7000 feet thick stacked reservoir unit sequence of shallow marine sands of cycle V and VI (Rahman et al., 2014; Johnson et al., 1989).

The offshore stratigraphy (Fig. 2) of the delta is characterized by occurrence of coastal to coastal-fluviomarine sand that have been deposited in a northwestwards prograding delta since the middle Miocene (from Cycle IV onwards (Fig. 2). The period of delta outbuilding are separated by rapid transgression, which are represented by marine shale intervals at the base of the sedimentary cycles (Fui, 1978). The regressive sands of each cycle grade northwestwards into neritic, mainly shaly sediments. Three major eustastically controlled cycles of regression and transgression have been described (Rijks, 1981). Each cycle develops in a coastal plain environment to the south, dominated by deposition of sands, silts and clays, and grades northward into holomarine neritic to bathyal environment with deposition of mainly clay, silt, minor sand in place turbidate. Twelve lithofacies were recognized within cycle V and VI of Middle to Upper Miocene based on lithology, sedimentary structures; degree of biotubation and fossils/trace fossils assemblage (Rahman et al., 2014).

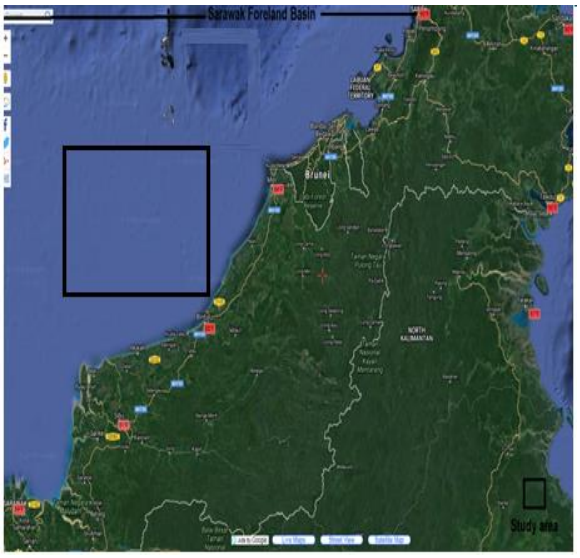

Fig. 1: Location of the Sarawak basin and the study area

The reservoir sandstones lithofacies identified are hummocky cross-stratified, Sweley cross-stratified, massive coarse, lenticular-bedded ribbon sand, interbedded laminated, interbedded laminated, laminated mudstone, heterogeneous, flasser bedded, shelly laminated, mud draped ripple laminated sandstones, silty, biotubated mudstone and muddy biotubated siltstone facies Rahman et al. (2014) were well described. The main reservoir sandstone units in West Baram Delta are within cycle V and VI in the Middle to Upper Miocene in geological age (Rahman et al., 2014; Ben-Awuah and Padmanabhan, 2014).

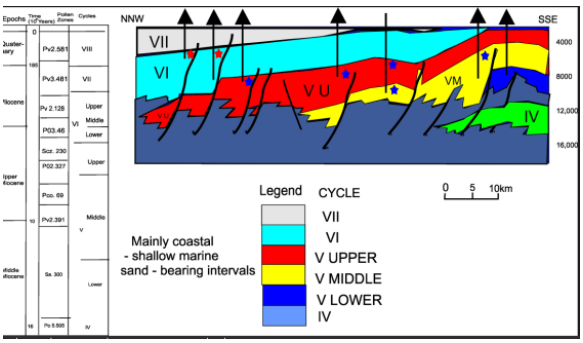

Fig. 2: Stratigraphy cross section of Baram Delta Province and some of study wells modified after (Hutchison, 2005)

3. Lithofacies description of studied samples

The studied specimen and core plugs were collected from five different exploratory wells; A, B, C, D and E, depicted in Fig. 3. The specimens are characterized into five lithofacies based on texture, sedimentary structure and trace fossil. The identified

lithofacies namely F1: massive coarse grained sandstone (MCGS); F2: massive medium grained sandstone (MMGS); F3: massive friable fine grained sandstone (MFFS); F4: massive fine grained sandstone (MFGS), and F5: massive very fine grained sandstone (MVFS).

The MCGS lithofacies is structure-less (Fig. 3a), coarse to medium grained, moderate to well-sorted grains, which suggests deposition in high energy wave dominated shallow marine (near shore) environment (Pettijohn et al., 1973). It is characterized with abundance of sub-rounded to well-rounded grains within lithofacies, which suggests indicative of farther away travelled sediments (Boggs, 2009).

Fig. 3: Representative specimen of (a) Massive coarse grained sandstone (MCGS) (b) Massive medium grained sandstone (MMGS) (c) Massive fine grained sandstone (MFGS) (d) Massive friable fine sandstone with embedded fossil fragments (MFFGS) and (e) massive very fine grained sandstone indicative of lamination (MVFGS)

The MMGS is poor to moderate well-sorted, intercalated with laminated silty mudstone parallel asymmetrical and symmetrical laminations with no biotubation features (Fig. 3b). It is characterized with sub-angular to rounded grains indicates deposition during less turbulent period in a wave- and storm dominated shelf, when the amount of sand rework and transport is greatly reduced (Boggs, 2009) suggests more than one depositional cycles.

The MFGS lithofacies is a fine to very fine grained, intercalated with subordinated mudstone. It is a poorly structured and appears to be homogeneous at macroscale level. It is characterize with biotubated burrows activities feature (Fig. 3c). It exhibits occurrence of sub-rounded to well-rounded grains indicative of deposition in quite wavy energy period (Boggs Jr and Krumbein, 1996).

The MFFS lithofacies is shelly laminated fining-upward sandstones and distinctive internal stratified (Fig. 3d). The basal part is planar laminated, medium to coarse grained sand with interbedded thin horizons of calcareous shell fragment grading upward into light grey, low- angle parallel laminated, fine grained sand. It is interpreted as a gutter cast, deposited during storm related to a relative sea-level fall, when oscillatory wave and wind-forced current scour shelf and cut deep gutter cast (Rahman et al., 2014).

The MVFS lithofacies consists of fine to very fine grained sandstones, with mudstone intraclasts scattered at the base of individual layers. It displays

low angle (< 15o) parallel to slight divergent stratifications (Fig. 3e). The texture suggests deposition in middle to upper shoreface environment dominated by storm and fair weather conditions, with long quiet periods (Rahman et al., 2014).

4. Material and methods

The study involves five exploratory wells (namely A, B, C, D and E) from three fields in the delta (Fig. 4). A total of 132 core sandstone specimens for lithofacies characterization and 97 (1.5 inches in diameter) core plugs sampled across the 5 wells have been used for the study. Core description and characterization was based on conventional textural and sedimentary structures (Boggs Jr and Krumbein, 1996). The sampled core specimens are dated as middle to upper Miocene in age, mainly with cycle IV and V stratigraphic succession.

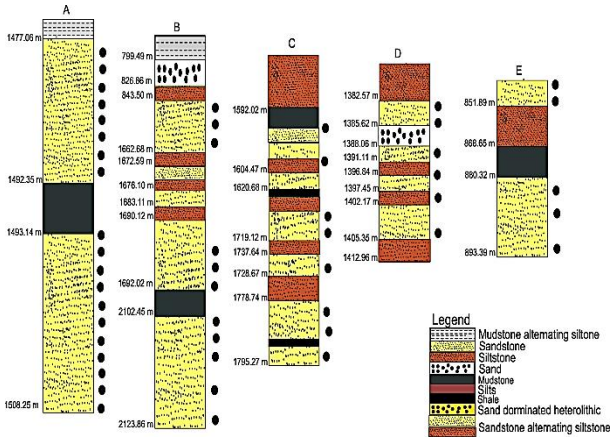

Fig. 4: Lithological core logs for sample points

The sample population from each lithofacies is: F1, n = 15; lithofacies F2, n = 21; lithofacies F3, n = 23; lithofacies F4, n = 19; lithofacies F5, n = 19 totaling to ninety seven (97). Each core specimen impregnated with blue epoxy dye into thin sections for petrographic extraction and quantification of petrofacies attributes such as grain shape, grain size, pore type and matrix are captured. Reservoir petrofacies is recognizing petrographic (De Ros and Goldberg, 2007; Kopaska-Merkel and Friedman, 1989) and petrophysical characteristics (Bhattacharya et al. 2005) that have greater impact on porosity and permeability (Savoy et al., 2000). Thin section analysis was carried out under polarized microscopy for grain-pore description each of the sandstone lithofacies under investigation. A 2D petrographic image analysis is use to extract and quantify grain-pore microscopic characteristics. Image J® Java-programmed application is used in analyzing various image-based samples (Aminu and Kulkarni, 2015) in this study.

The digitally generated outputs for grain shape, grain size were converted to millimeter (mm) from (µm) using Udden-Wentworth geometric sedimentological scale (Udden, 1914; Wentworth, 1922) for sediment and equivalent phi (Φ) scale (Figs. 10, 12, and 13). Quantification of pore types are characterized into interparticle, intraparticle and fracture pores from visual 500 point count.

A core slabs of 2cm by 2cm from specimen taken to visualize and examine (Welton, 1984) grain-pore diagenetic relationship in an undisturbed state using scanning electron microscopy (SEM) model Carl Zeiss Supra 55 instrument operates at variable pressure varying from 2pa to 133pa with a probe current between 1pA to 10nA having amplification varying from ×100 to ×10000 µm were used.

Permeability and porosity measurement was determine using Coreval 30 helium porosimetry equipment on core plugs of 1.5 inches in diameter according to the American Petroleum Institute recommendation practice 40 (API RP 40) at a maximum confining pressure of 400psi. The equipment measures permeability between 0.001md and 10D, porosity up to 60 %. Permeability to gas tests was performed using unsteady-state pressure fall-off technique.

The analysis of fluid flow lateral extent and continuity was evaluated using statistical hierarchical cluster analysis (Knofczynski and Mundfrom, 2008; Petrocelli, 2003), and their output is presented in pictorial dendrogram for the five wells; as vertical axes shows different sandstone lithofacies description and horizontal axes shows dissimilarity coefficient between the different petrofacies/porosity-permeability clusters. Tabulated average summaries of each petrofacies/ porosity-permeability clusters in each studied wells are correlated to understand changes and variations in fluid flow characteristic (porosity and permeability) lateral extent and continuity with variable depth from the near shore well C to the farthest well B in prodelta of the study offshore wells.

5. Results and discussions

5.1. Petrography description of studied representative samples

5.1.1. Massive coarse grained sandstone (MCGS)

MCGS lithofacies (Fig. 5) show quartz as most abundant mineral fraction. This mineral are majorly of variable grain size and shapes, having total composition of 48.74% comprises of both monocrystalline quartz and very coarse polycrystalline quartz (Figs. 5a-5b) at different grain orientation.

The polycrystalline quartz exhibits multiple fractures ascribed to effect of hydrostatic water pressure and tectonic event that have occurred in the delta (Tan et al., 1999). The straight quartz boundary are most predominant associated to moderate compaction at depths (Boggs Jr and Krumbein, 1996) indicated by lesser occurrence of suture grain contacts in this lithofacies. The straight grain boundary suggests that the quartz grain are of igneous rock origin (Adams et al., 2017). Also this

lithofacies is characterize with minor amount of matrix composition at 7.79% less than 15% fine grained matrix for greywacke sandstone classification (Boggs, 2009). While in some lithofacies members completely obliterate intergranular spaces (Fig. 5b) of the framework suggest features of low depositional energy environment (Boggs, 2009) and indicative of more than one single cycle. Quartz grains are moderately sorted, varying in size from 298µm to 612µm grain size, and the total intergranular average pore size varies between 89µm and 282 µm suggest attributed to moderate compaction and minor pore-filling matrix (Boggs, 2009). The wide range in grain shapes are associated to sediment transport process defined by relative farther or nearer from the sources (Pettijohn et al., 1973).The sub-rounded to rounded grain are the most predominant shapes (Fig. 10) in the sample than angular to sub-angular grains present. Predominant grain packing are the float and point contacts, with very sparse to non-availability of long, concavo-convex and suture packing associated to moderate compaction exerted by column hydrostatic pressure of the water (Boggs, 2009). The sediment size, sorting transport mode and flow velocity may all suggest affects grain orientation as it varies as 10.4% (0o- 30o), 24.50% (31o- 60o), 9.50% (61o-90 o), 14.70% (91o-120o), 24.80% (121o-150o and 16.10% (151o-180o). The MCGS lithofacies suggest deposition in high energy wave environment with moderate grain compaction and exhibit abundance of intergranular pore space associated to minor matrix composition.

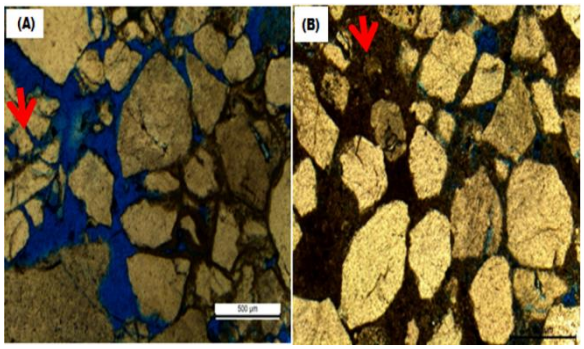

Fig. 5: representative thin sections of thin sections for MCGS sandstone lithofacies (Well C-C5B3) at depth 1334.9m (a) grain-pore composition (b) depicted obliterated intergranular pore space by fine fraction

5.1.2. Massive medium grained sandstone (MMGS)

In MMGS lithofacies (Fig. 6) abundant quartz mineral are monocrystalline grains, with moderate occurrence of polycrystalline grain of 38% total composition.

They exhibits straight grain boundary indicative of igneous source (Adams et al., 2017) grain, and contain high matrix of 31% composition indicative of low wave energy environment of deposition (Pettijohn et al., 1973). They also comprise of 18% intergranular porosity ascribed pore reduction by pore-filling matrix obliterates intergranular pore spaces (Morad et al., 2000). The minor monocrystalline angular to sub-angular grains are prominent grain shapes (Fig. 10) ascribed to possibly short distance travels by sediment (Boggs, 2009) from source. The grains size varies from 18.23µm to 121.2 µm therein include rounded and sub-rounded grains indicative of farther distance travelled sediments, suggest occurs in more than one single cycle depositional energy in the delta (Boggs, 2009). The grains are moderate to well sorted grains, having mixed abundance of point over float contacts indicative of a moderate more compaction than MCGS lithofacies. It exhibits also moderate occurrence of straight boundary over suture grain boundary. The grains are oriented between angles 31o - 90o (29%) and 120o - 180o (37%) within the framework.

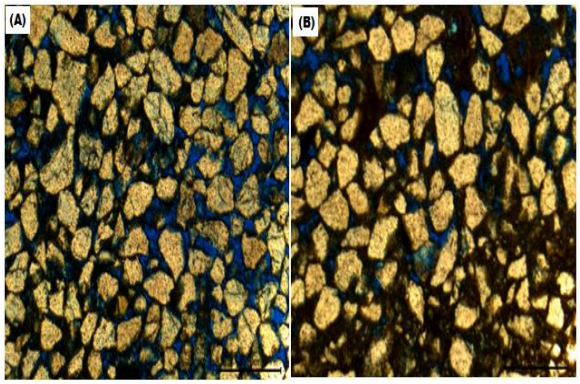

Fig. 6: representative thin section of for MMGS sandstone lithofacies C- C14T9 at depth 1771.2m (a) depicted section abundance of pore supportive grains (b) section reveals intergranular pore obliterated by fine fractions

5.1.3. Massive fine grained sandstone (MFGS)

In MFGS (Fig. 7) lithofacies comprises of medium to fine grain quartz. The grain crystals are majorly monocrystalline quartz. These contain some moderate occurrence of random coarse quartz grains within the lithofacies framework, indicative of more than one single depositional cycle (Pettijohn et al., 1973). The random coarse grain is attributed to intrusion of coastal to coastal-fluviomarine sand which have been deposited in a northwestwards prograding delta since the Middle Miocene (from Cycle IV onwards) (Tan et al., 1999). Quartz grain mineral made up 45.91% of total grain composition with an intergranular porosity of 28.18% enhance by occurrence of float and point contact packing (Figs. 7a and 7b). The pore sizes in this lithofacies vary from 4.12µm to 43µm. The grain sizes varies from 1.12µm - 82µm exhibit high occurrence of sub-rounded, rounded and sub angular grains within the framework, this ascribed farther distance traveled by the sediments (Boggs, 2009).

In this lithofacies, grain distributions varies from poorly sorted to moderately sorted with predominantly float and point contacts packing (Figs. 7a and 7b). Long and concavo-convex contacts are minimal with abundant of their grains oriented

at angles between 31°- 60° and 121°-151° at 24.60% and 19.40% respectively.

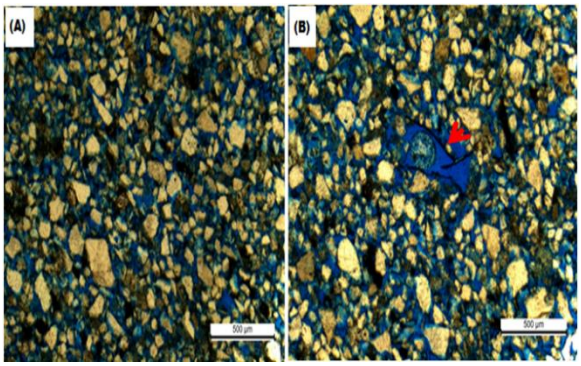

Fig. 7: show representative thin section for MFGS sandstone lithofacies Well C 21C2B14 at depth 1365.7m (a) Depicted variable size rounded fine and random coarse grains (b) mesopore pore depicted by red arrow within the framework

5.1.4. Massive friable fine grained sandstone (MFFGS)

In this lithofacies (Fig. 8) quartz mineral and fine grained sand including silts forms the dominant part of the framework. The intercalation of monocrystalline coarse-fine grained forming lamina/lamination depicted with red arrows (Fig. 8a). The monocrystalline quartz mineral and fine grained matrix made up 21% and 48% respectively in the framework. The quartz grain shows straight boundary contacts indicative of igneous rock source, void of suture grain contacts. This also suggests a moderate compaction due to overlying hydrostatic or lithostatic pressure within the delta. The lithofacies exhibit both intergranular and narrowly matrix-fracture (Fig. 8b) ascribed to increase in confining pore pressure and temperature with depth (Nelson and Handin, 1977) exhibit average porosity of 18% within framework. Angular to sub-angular grains are predominant grain and moderate composition of sub-rounded grains exhibits distribution varying from poorly to moderate sorted grain. In this lithofacies, predominant grain contacts are long and float contact. It grains within framework are oriented at angles above 100°, but less than 180°.

5.1.5. Massive very fine grained sandstone (MVFS)

I n MVFS lithofacies (Fig. 9) contains highest volume of matrix and fine fraction composition compared to lithofacies. The framework comprise of coarse monocrystalline quartz grain 26% suggest ascribed to intrusion of coastal to coastal-fluviomarine sand which have been deposited in a northwestwards prograding delta since the Middle Miocene (from Cycle IV onwards) (Tan et al., 1999) during depositional regime.

The lithofacies comprise of matrix content up to 58% attributed deposition in a low to quite energy environment (Boggs, 2009). Intergranular porosity are obliterated by fine fractions (Fig. 9a), but exhibits abundance of matrix-fracture (Nelson, 2001), (Fig. 9b) suggest attributed to increase in confining pore pressure and temperature with depths that exist within reservoir stratigraphic units.

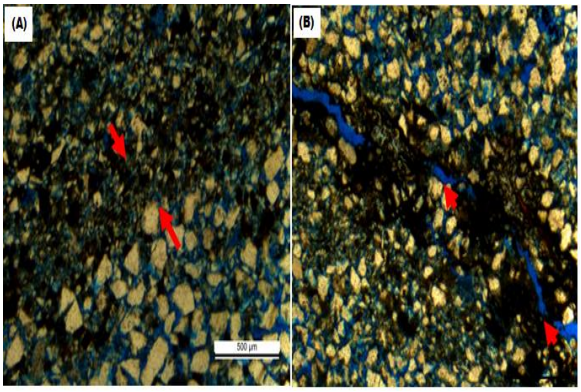

Fig. 8: representative thin sections of thin sections for MFFGS sandstone lithofacies (WL4C18T3) at 1502m (a) coarse-fine grained lamina depicted with long red arrow (b) depicted matrix-fracture porosity

This lithofacies comprise abundance of subangular, sub-rounded to rounded grains ascribed to farther distance traveled by sediments into relatively low energy environment (Boggs Jr and Krumbein, 1996). Grain distribution in this lithofacies varies from moderate to poorly sorted grain ascribed to depositional environment and relative farther or nearer from the sources (Pettijohn et al., 1973). It exhibit abundance of point and concavo-convex contacts, but moderate occurrence of long contacts. Grains vary in sizes from 38µm to 279µm dominantly oriented at angles less than 100o within framework. The analysis indicates an abundant porosity supportive characteristic ascribed to occurrence coarse and medium sub-rounded, rounded and well-rounded grains within studied lithofacies including the fine grained lithofacies introduced by occurrence of coastal to coastal-fluviomarine sand which have been deposited in a northwestwards prograding delta since the Middle Miocene (from Cycle IV onwards) (Tan et al., 1999) during depositional regime. Intergranular porosities are obliterated by matrix content in coarse and medium grained lithofacies, exhibit abundance of matrix-fracture pores ascribed to increase in temperature at depth and confining pore pressure (Nelson and Handin, 1977).

5.2. 2D image quantification of petrofacies attributes from thin sections

Reservoir petrofacies is recognizing petrographic (De Ros and Goldberg, 2007; Kopaska-Merkel and Friedman, 1989) and petrophysical characteristics (Bhattacharya et al., 2005) attributes in samples that have greater impact on porosity and permeability (Savoy et al., 2000). The textural grain-pore compositions extracted from 2D digital images analysis and quantified using (Wentworth, 1922)

sedimentological scale in all studied 5 sandstone lithofacies. The sixteen (16) textural composition variables in percentage (%) includes granules, very coarse sand, coarse sand, medium sand, fine sand, fine silts, coarse silts, clay, very angular grain, angular grain, sub-angular grain, sub-rounded grain, rounded grain, well-rounded grain and porosity.

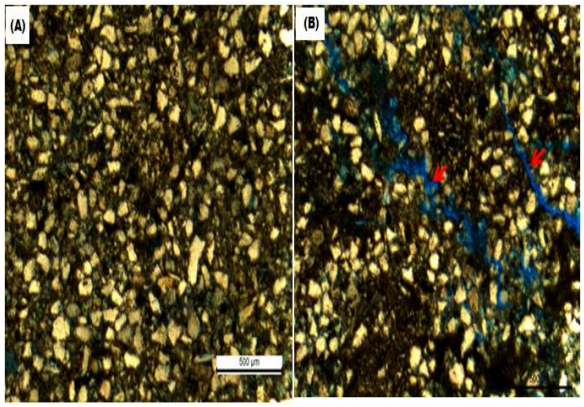

Fig. 9: representative thin sections for MVFGS sandstone lithofacies at WL4C12T18 at 895.2m (a) depicted fine grained with high fine fractions with random coarse and medium grains (b) matrix-fracture porosity depicted by red arrows in the framework

5.2.1. Grain shapes and pore type's distribution in studied lithofacies

From Fig. 10, massive coarse grained sandstone (MCGS) and massive medium grained sandstone (MMGS) lithofacies, both exhibits minimal abundance of very angular grains, but are moderate in massive fine grained sandstone (MFGS) compare to massive medium fine grained sandstone (MMFGS) and massive very fine grained sandstone (MVFGS).

There are uneven distributions of angular grains, MCGS closely in abundance with MFGS lithofacies. It is minimal in MMGS and moderate in abundant for MFFGS and MVFG.

The sub-angular grains are abundance in MVFG and MFGS and moderately higher in MFFGS and MMGS as related to MCGS. The composition abundance of sub-rounded and rounded grains vary across in all the lithofacies, increasingly in MFGS, MCGS, MFFGS, MVFGS and MMGS, while well-rounded grains increases in MCGS, MMGS, MVFGS as compare to MFFGS and MFGS. The variable abundance of grain shapes differ proportion volume of interparticle pores vary, but higher in MCGS, then in MMGS, MVFGS, MFGS and MFFGS lithofacies. It indicates that all studied sandstone lithofacies exhibits abundant supportive grain-pore attributes compositions, potentially ascribed to occurrence of coastal to coastal-fluviomarine sand which have been deposited in a northwestwards prograding delta since the Middle Miocene (from Cycle IV onwards) (Tan et al., 1999) during depositional regime have improved microscopic reservoir properties across sandstone lithofacies.

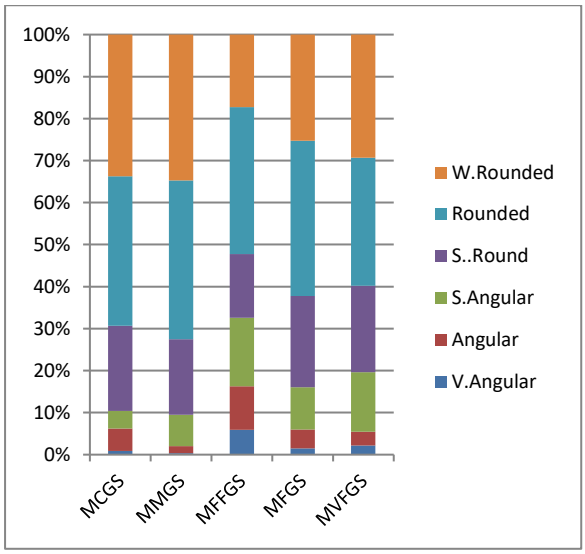

Fig. 10: Grain shapes distribution in sandstone lithofacies Baram Delta

SEM microphotographs (Fig. 11), showing common depositional and diagenetic features that modifies pore attribute characteristics in the different sandstone lithofacies from the West Baram Delta. Different parts of Fig. 11 are as below:

a) Medium grained sandstone with kaolinite occluding pores
b) lower magnification of kaolinite in a pore
c) Coarse grained with fine fractions randomly clogging pores
d) indicates fine fraction filling and clogging pore and throat
e) Fine grained sandstone with high fine fractions filling intergranular pore spaces with granule size grains
f) and (g) Coarse grained sandstone with grain-pore supportive sizes and shapes with random dispersal of fine fractions clogging pores and throats

From Fig. 12, present distribution of micropores and mesopores in studied sandstone lithofacies from 2D image analysis according to Loucks et al. (2012) classification. Intraparticle pore are abundance in MFFGS suggest to occurrence of fossil shell fragment (Fig. 11e) and in MVFG extensive tectonic regime (Tan et al., 1999) result in occurrence of fracture pores (Fig. 6a) at different proportion across studied lithofacies suggests to enhance abundance of mesopore (Nelson, 2001).

Also, occurrence of wide matrix-fracture in massive fine grained lithofacies (Figs. 9-10b) ascribed to increase in temperature and confining pore pressure at depth (Nelson and Handin, 1977) in overpressure delta. However, but in MMGS and MCGS lithofacies exhibits minimal occurrence, due to less fine grained fraction enhance abundance of intergranular porosity (Fig. 11a-11f).

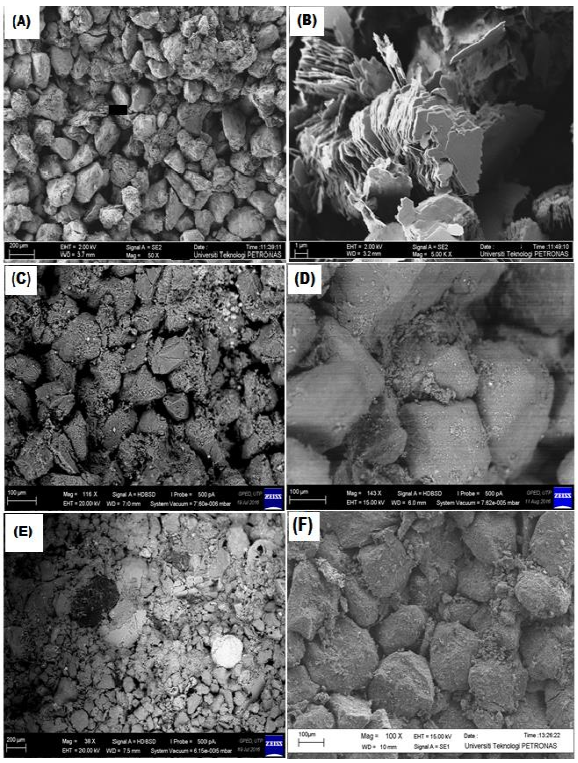

Fig. 11: SEM Photomicrographs showing common depositional and diagenetic features that indicate role played by grains compositions to pores/fluid characteristics in the different sandstone lithofacies from West Baram Delta.

Fracture pores are prominent in MFGS and MMGS, but moderately in MCGS and MFGS (Fig. 12). The occurrence of variable grain shapes (Fig. 13) contribute to development of different percentage of pore types (Fig. 12).

The different grain shapes and volume of fine fractions associated to distance traveled by sediments closer or farther to source by hydrodynamic energy in era of deposition (Boggs, 2009; Pettijohn et al., 1973). The analysis indicates that most of the lithofacies with abundance of sub-round, rounded and well-rounded grains potentially facilitates occurrence of intergranular mesopores (Fig. 12).

The percentage composition of clays, silts and fine grained sand fractions (Fig. 13) present at variable proportion occlude and clog pores and structure (Figs. 11b-11d). These necessitate increase in abundance of micropores over mesopores in MFGS and MVFGS lithofacies (Fig. 12) clogging interparticle and pore-throat (Figs. 11c-11f). The combined admixture of the variable proportion of grain shapes distributions varies pore attributes and fluid flow (Ehrlich et al., 1997; McCreesh et al., 1991) distribution.

5.3. Evaluation of petrofacies distribution in West Baram Delta, Offshore Sarawak

The petrographic reservoir petrofacies grain-pore composition quantified that have greater impact on porosity and permeability (Savoy et al., 2000) in reservoir sandstone lithofacies. The sixteen (16) textural composition variables in percentage (%) and permeability data in studied reservoir sandstone lithofacies are statistically discriminated into different petrofacies clusters within well and across all wells. The results are presented in coloured dendogram to reveal relation between different reservoir sandstone lithofacies at depths, as petrofacies clusters with same colours belong in similar cluster exhibits similar porosity and permeability distribution (Figs. 14-18).

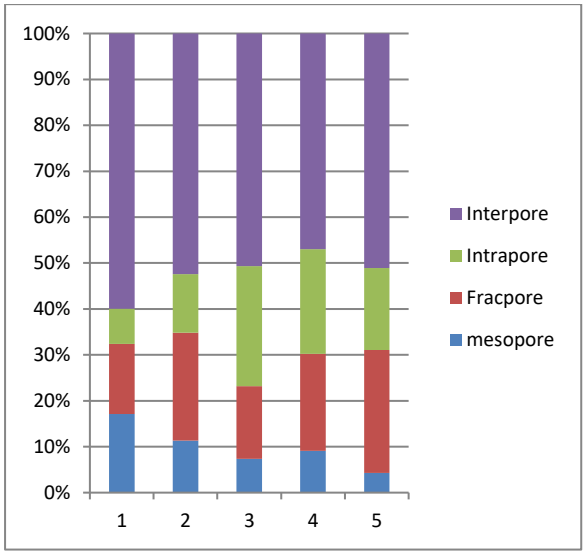

Fig. 12: distribution of micropores and mesopores in studied sandstone lithofacies from 2D image analysis using (Loucks et al., 2012) classifications

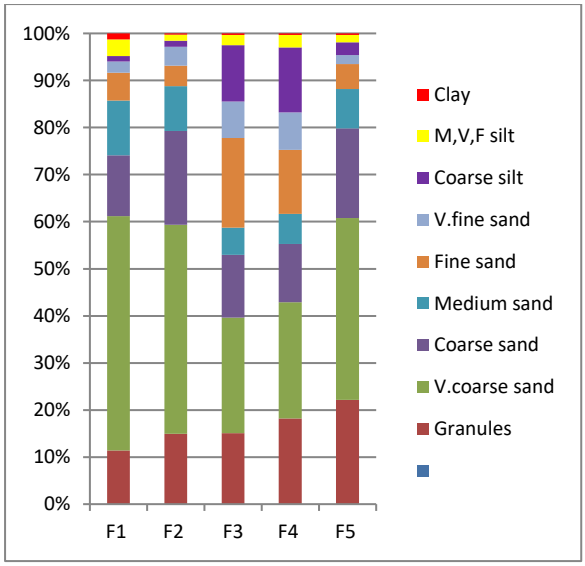

Fig. 13: Mean composition value in lithofacies based on Udden-Wentworth grain-size scale for sediment and the equivalent phi (Φ) scale

5.3.1. Well A

In well A, comprise of four petrofacies clusters namely green, brown; yellow and blue (Fig. 14). The green and red petrofacies cluster are closely very similar in porosity and permeability composition indicated by horizontal coefficient of less than 5, characterized by massive medium grained and massive fined grained sandstone lithofacies at depth

from 1482 m - 1508 m exhibits average porosity between 16% - 19% and permeability 140 mD - 210 mD. While, the yellow and blue petrofacies clusters at depth from 1488 m to 1904 m characterized by massive coarse grained and massive friable fine grained sandstone lithofacies with porosity between 29% - 32% and permeability 480 mD - 1920 mD indicates moderate dissimilarity with green and red petrofacies clusters depict by horizontal coefficient slightly above 5. It shows that red, yellow and blue petrofacies dominated by coarse and medium sand grains exhibits moderate high porosity and permeability (Tiab and Donaldson, 2015). However, decrease in porosity and permeability distribution in green and brown petrofacies clusters suggest ascribed to abundance fine-very fine sand at the section, whereas increase in these properties in yellow and blue petrofacies clusters attributed to coarse - very coarse grain, well-rounded grains around depth 1488m-1904m.

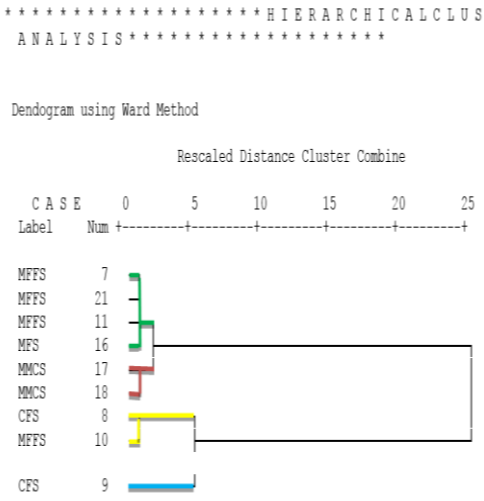

Fig. 14: showing "A" well petrofacies clusters dendogram

5.3.2. Well B

In well B, four petrofacies clusters namely green, brown, yellow and blue clusters (Fig. 15). The green and brown clusters are characterize by massive friable fine grained and massive medium grained sandstone lithofacies at depth from 2096m - 2125m comprises of porosity between 14%-27% and permeability between 423mD - 657mD, while at depth 2095m-2129m in yellow and blue petrofacies clusters; porosity varies from 14% - 25% with permeability varying between 10mD to 1189mD within massive fine grained sandstone lithofacies. These variations are attributed to grain-pore composition changes that occurs within the different lithofacies clusters sourced from different depositional systems in the well.

5.3.3. Well E

In well E, three petrofacies clusters are identified namely green, brown and blue (Fig. 16). The green cluster at depth 880m - 891m are characterize mainly by massive very fine grained sandstone lithofacies with porosity between 15% -27% and permeability from 110mD to 840mD. The horizontal dissimilarity coefficient of less than 5 is good, because of their similarity in depositional system. The brown petrofacies cluster characterize by massive fine grained sandstones, but differs at depth from 889-893m in porosity between 18% - 22% and permeability from 330 mD to 420mD in green petrofacies cluster with coefficient value greater than 5, and this could be ascribe to coastal-coastal-fluviomarine sand sediments deposited in a northwestwards (Tan et al., 1999) supporting porosity and permeability within fine grained lithofacies (i.e., coarse or medium rounded, well-rounded grains) in the study area. While in the blue petrofacies cluster characterize by massive fine grained sandstone at depth of 859m exhibits porosity of 21% and permeability 840mD. This cluster reveals the largest dissimilarity coefficient above 20 compared green and brown petrofacies clusters.

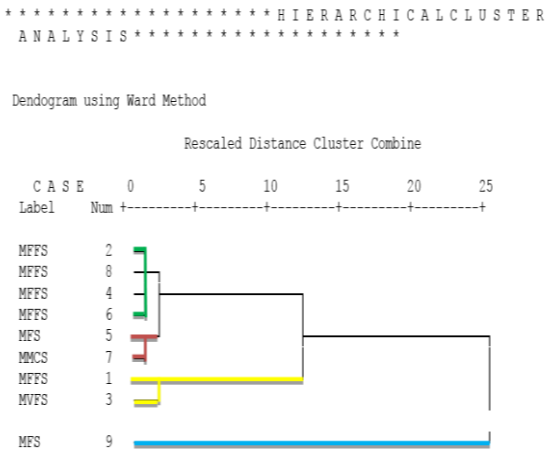

Fig. 15: showing "B" well petrofacies clusters dendogram

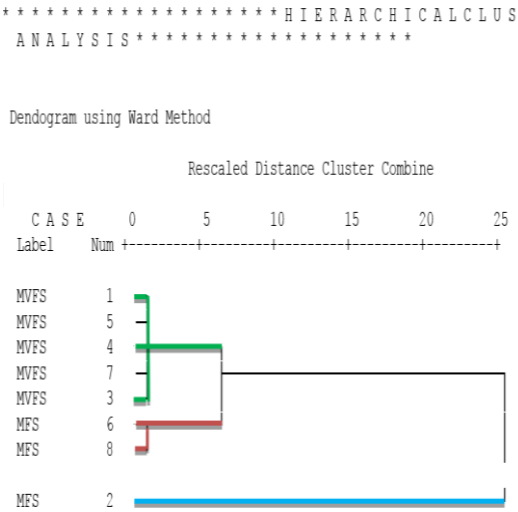

Fig. 16: Showing "E" well petrofacies clusters dendogram

5.3.4. Well D

In well D, two distinct petrofacies clusters of green and blue are identified in this well (Fig. 17). The green petrofacies cluster is characterized with massive medium grained sandstone at depth 1391m-1398m. This cluster exhibit 25% - 30% porosity and permeability between 567mD - 670mD, with horizontal dissimilarity coefficient less than 5 indicative of good relation within cluster. The blue cluster is characterize by massive very fine grained sandstone at depth from 1381m-1406m shows porosity between 21% - 26%, permeability from 400mD to 435mD.

In the blue petrofacies cluster, horizontal coefficient is greater than 5 and less than 10. It is indicates that green cluster are closely related, than those in the blue cluster.

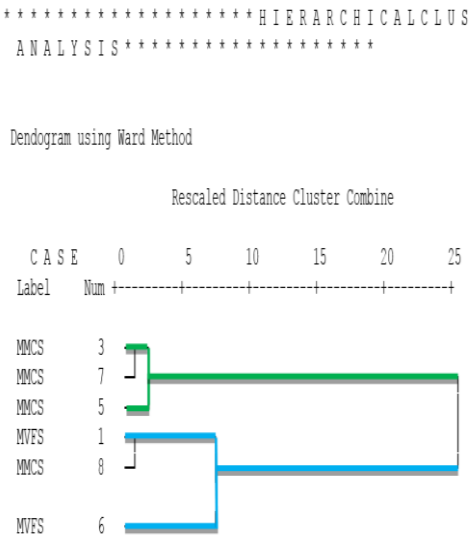

Fig. 17: showing "D" well petrofacies clusters dendogram

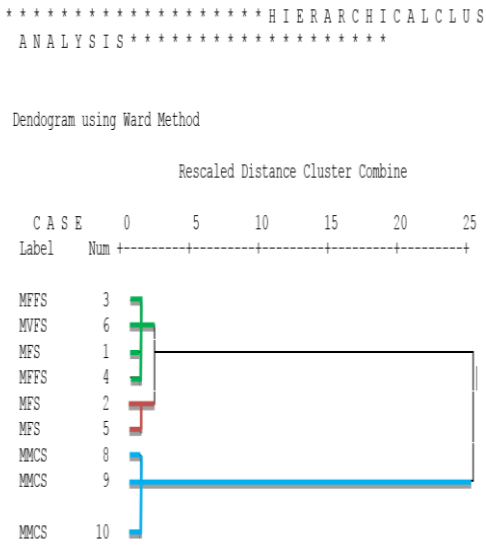

Fig. 18: showing "C" well petrofacies clusters dendogram

5.3.5. Well C

In well C, three clusters are identified namely green, brown and blue petrofacies clusters (Fig. 18). The green petrofacies cluster is characterized by massive fine grained sandstone, but dominant of massive friable fine grained sandstone lithofacies at from depth 1720m-1805m. In this cluster exhibit horizontal coefficient less than 5 and porosity vary from 15%-22% and permeability vary from 120mD-220mD. While, the brown petrofacies cluster at depth 1730m-1800m is characterized also by massive fine grained sandstone, exhibit porosity varying between 18% -19% and permeability between 330mD-343mD in the well. The two petrofacies clusters shows low horizontal coefficient of 3 indicative of close similarity in depositional system and so in petrophysical properties. The blue petrofacies cluster is characterize by mainly massive medium grained sandstone at depth 1815m -1825m and porosity between 18% - 25% and permeability between 720 mD - 945 mD within the cluster.

5.4. Delineation of reservoir petrofacies lateral continuity for flow zones in wells

Reservoir petrofacies discrimination are evaluated and summarized based on grain composition, porosity in percentage and permeability data in mD are used to delineate lateral extent of flow zone continuity. The average summaries of the petrofacies clusters in each studied wells from summarized in Table 1-5 are correlated to understood changes and variations in lateral fluid flow characteristic (porosity and permeability) with depths from near shore well "C" to the farthest Well "B" in prodelta of the study offshore wells. This determines petrofacies cluster(s) with good reservoir quality fluid flow properties of consistent geometric spread across the wells for an effective areal sweep efficiency during hydrocarbon recovery.

Table 1: Summary of petrofacies cluster for Well C

Cluster	Depth(m)	Porosity (%)	Permeability (mD)
Green petrofacies	1720 - 1805	15-22	120 -220
Brown petrofacies	1730 - 1800	18 -19	330-343
Yellow petrofacies	Nil	Nil	Nil
Blue petrofacies	1815 - 1825	18-25	720-945

Table 2: Summary of petrofacies cluster for Well A

Cluster	Depth(m)	Porosity (%)	Permeability (mD)
Green petrofacies	1482	16	140
Brown petrofacies	1508	19	210
Yellow petrofacies	1488	29	480
Blue petrofacies	1904	32	1920

Table 3: Summary of petrofacies cluster for Well E

Cluster	Depth(m)	Porosity (%)	Permeability (mD)
Green petrofacies	880-891	15-27	110-840
Brown petrofacies	889-893	18-22	330-420
Yellow petrofacies	Nil	Nil	Nil
Blue petrofacies	859	21	840

Table 4: Summary of petrofacies cluster for Well D

Cluster	Depth(m)	Porosity (%)	Permeability (mD)
Green petrofacies	1391-1398	25-30	567-670
Brown petrofacies	Nil	Nil	Nil
Yellow petrofacies	Nil	Nil	Nil
Blue petrofacies	1381-1406	21-26	400-435

Table 5: Summary of petrofacies cluster for Well B

Cluster	Depth(m)	Porosity (%)	Permeability (mD)
Green petrofacies	2096-2125	14-27	423-526
Brown petrofacies	2110-2122	24-25	600-657
Yellow petrofacies	2095-2099	14-22	10-243
Blue petrofacies	2129	25	1189

The essential fluid flow properties of reservoir rocks are porosity and permeability of sandstone lithofacies for conventional resource plays (Amaefule et al., 1993). From well "C", the green petrofacies clusters mainly characterized by massive fine grained sandstone, massive friable fine grained sandstones, massive very fine grained sandstone and massive medium grain sandstone lithofacies across studied wells into the A, E, D and B wells at variable depths. The changes and variations in the petrofacies cluster porosity and permeability is attributed to grain-pore attribute composition (Table 1-5).

Reservoir lateral extent and continuity in the order of well placement (Fig. 19) reveals that the Green petrofacies cluster from moderate deep (W-C) well in west near shoreface at depth 1780m exhibit maximum porosity of 22% and permeability of 220 mD extend to (W-A) well at depth 1482 m with decreasing porosity of 16% and permeability of 140mD. This also extend eastward into shallow W-E well that exhibit moderate increase in porosity up to 27% and permeability of 840 mD progressively into W-D well reveals maximum of 30% porosity and permeability increases up to 670 mD. Farther away into prodelta, (W-B) well at deeper depth at 2125m exhibit slight decrease in porosity to 27% and permeability of 526 mD.

In the Brown petrofacies clusters, lateral connectivity from near shoreface (W-C) well at depth 1730 m exhibits slight decrease in porosity to 19% than in the Green petrofacies cluster, but reveals moderate increase in permeability to 343 mD in this well. It extends into W-A well at depth of 1508m to maintain maximum porosity, with slight decrease in permeability to 210mD. At depth 889 m, in shallow in the W-E well, porosity and permeability slightly increases to 22% and 420mD into farthest W-B well that exhibits porosity and permeability of 25% and 657mD respectively as it is missing in the (W-D) well probably due to extreme faulting and tectonic event (Fig. 2) that have occurred in the West Baram Delta (Tan et al. 1999).

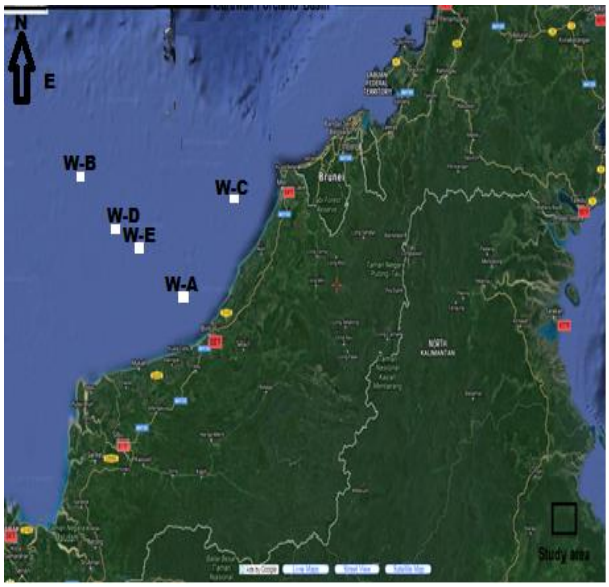

Fig. 19: showing studied wells layout in West Baram Delta

Furthermore, lateral extent in the Yellow petrofacies clusters are missing in the wells; W-C, W-E and W-D except in the farther away from shoreface (W-A) well at depth 1488 m exhibit porosity of 29% and permeability value up to 480 mD extending into prodelta W-B well at depth 2099 m exhibit decrease in porosity to 22% and permeability to 234 mD. Reservoir lateral extent and continuity within the Blue petrofacies cluster from the (W-C) well at depth 1825 m exhibits 25% porosity and permeability of 945 mD extending into (W-A) well southeast reveals moderate increase in porosity to 32% and permeability to 1920 mD at depth of 1904 m. The porosity and permeability slightly decreases to 12% and 840 mD respectively in shallow W-E well at depth of 859m. But further decreases in permeability to 435mD into the (W-D) well at depth 1406 m and increase into prodelta (W-B) well at deeper depth of 2129 m exhibits maximum permeability of 1189 mD. It indicates porosity and permeability improves with depths and distance into prodelta as grain-pore composition attributes improves in the Blue, followed by Green and Brown petrofacies across the five wells.

6. Conclusion

Reservoir lateral extent and continuity was evaluated using statistical hierarchical analysis through integration of petrographic, 2D digital image analysis, scanning electron microscope (SEM) and helium porosimetry data. The result reveals four main petrofacies clusters of similar lateral extent

and continuity are the Blue petrofacies cluster characterized with massive coarse grained sandstones, massive fine grained sandstones and massive very fine grained sandstone lithofacies, followed by Green dominated by massive friable fine grained sandstone, massive very fine grained sandstone and massive medium grained sandstone lithofacies and the Brown petrofacies comprise of massive medium grained and massive fine grained sandstone lithofacies clusters exhibits good reservoir quality and lateral continuity of similar porosity and permeability distribution at different depths in all studied wells. It reveals that their lateral continuum in grain-pore composition for porosity - permeability improves farther away into prograding delta of the West Baram Delta. This technique could be applicable for quick delineation of fluid flow lateral extent and continuity between wells to improve field design for effective areal sweep efficiency of hydrocarbon during reservoir flooding.

Acknowledgement

This research was supported by Universiti Teknologi PETRONAS, Malaysia under Graduate Assistantship Scheme. The author would like to thank PETRONAS for providing me with PhD scholarship opportunity and subsurface core specimens for this work.

Compliance with ethical standards

Conflict of interest

The authors declare that they have no conflict of interest.

References

Abu Bakar M, Yeap YC, Nasir E, Din A, Chai CF, Adamson GR, and Valdez R (2011). EOR evaluation for Baram delta operations fields, Malaysia. In the SPE Enhanced Oil Recovery Conference, Society of Petroleum Engineers, Kuala Lumpur, Malaysia. https://doi.org/10.2118/144533-MS

Adams AE, MacKenzie WS, and Guilford C (2017). Atlas of sedimentary rocks under the microscope. Routledge, Abingdon, UK. https://doi.org/10.4324/9781315841243

Amaefule JO, Altunbay M, Tiab D, Kersey DG, and Keelan DK (1993). Enhanced reservoir description: Using core and log data to identify hydraulic (flow) units and predict permeability in uncored intervals/wells. In the SPE Annual Technical Conference and Exhibition, Society of Petroleum Engineers, Houston, USA: 205-220.

Aminu MD and Kulkarni KS (2015). The influence of grain morphology on reservoir quality of some Athabasca oil sands samples. Journal of Geology and Geophysics, 4(3): 1-5.

Bear J and Bachmat Y (2012). Introduction to modeling of transport phenomena in porous media. Vol. 4, Springer Science and Business Media, Berlin, Germany. **PMCid:PMC3282414**

Ben-Awuah J and Padmanabhan E (2014). Porosity and permeability modification by diagenetic processes in fossilferous sandstones of the West Baram Delta, offshore Sarawak. International Journal of Petroleum and Geoscience Engineering, 2(2): 151-170.

Ben-Awuah J, Padmanabhan E, Andriamihaja S, Amponsah PO, and Ibrahim Y (2016). Petrophysical and reservoir characteristics of sedimentary rocks from offshore west Baram delta, sarawak basin, Malaysia. Petroleum and Coal, 58(4): 414-429.

Bhattacharya S, Doveton JH, Carr TR, Guy WR, and Gerlach PM (2005). Integrated core-log petrofacies analysis in the construction of a reservoir geomodel: A case study of a mature Mississippian carbonate reservoir using limited data. AAPG Bulletin, 89(10): 1257-1274. https://doi.org/10.1306/06030504144

Boggs Jr S and Krumbein WE (1996). Principles of sedimentology and stratigraphy. Sedimentary Geology, 105(1): 112-114.

Boggs JS (2009). Petrology of sedimentary rocks. Cambridge University Press, Cambridge, UK. https://doi.org/10.1017/CBO9780511626487

Darman NB, Samsudin Y, and Sudirman S (2007). Planning for regional EOR pilot for Baram delta, offshore Sarawak, Malaysia: Case study, lesson learnt and way forward. In the Asia Pacific Oil and Gas Conference and Exhibition. Society of Petroleum Engineers, Jakarta, Indonesia. https://doi.org/10.2118/109220-MS

De Ros LF and Goldberg K (2007). Reservoir petrofacies: A tool for quality characterization and prediction. In the AAPG, Annual Convention and Exhibition, Long Beach, California: 1-7.

Ebanks WJ (1987). Geology in enhanced oil recovery. The Society of Economic Paleontologists and Mineralogists, New York, USA. https://doi.org/10.2110/pec.87.40.0001

Ehrlich R, Prince C, and Carr MB (1997). Sandstone reservoir assessment and production is fundamentally affected by properties of a characteristic porous microfabric. In the SPE Annual Technical Conference and Exhibition, Society of Petroleum Engineers, Antonio, USA: 591-599. https://doi.org/10.2118/38712-MS

Fui HK (1978). Stratigraphic framework for oil exploration in Sarawak. Geological Society of Malaysia Bulletin, (10): 1-13.

Henares S, Caracciolo L, Cultrone G, Fernández J, and Viseras C (2014). The role of diagenesis and depositional facies on pore system evolution in a Triassic outcrop analogue (SE Spain). Marine and Petroleum Geology, 51: 136-151. https://doi.org/10.1016/j.marpetgeo.2013.12.004

Hutchison CS (2005). Geology of north-west borneo: Sarawak, Brunei and Sabah. Elsevier, New York, USA.

Johnson HD, Kuud T, and Dundang A (1989). Sedimentology and reservoir geology of the Betty field, Baram Delta Province, offshore Sarawak, NW Borneo. Geological Society of Malaysia Bulletin, 25: 119-161.

Knofczynski GT and Mundfrom D (2008). Sample sizes when using multiple linear regression for prediction. Educational and Psychological Measurement, 68(3): 431-442. https://doi.org/10.1177/0013164407310131

Kopaska-Merkel DC and Friedman GM (1989). Petrofacies analysis of carbonate rocks: Example from lower Paleozoic Hunton Group of Oklahoma and Texas. AAPG Bulletin, 73(11): 1289-1306.

Latief AI, Ridzuan AI, Faehrmann PA, Macdonald AC, Arina W, and Rahman G (2012). An innovative static modeling approach to handle a complex giant within a compressed timeframe; A case study of Baram oil field, offshore Sarawak, East Malaysia. In the SPE Asia Pacific Oil and Gas Conference and Exhibition, Society of Petroleum Engineers, Perth, Australia. https://doi.org/10.2118/159532-MS

Loucks RG, Reed RM, Ruppel SC, and Hammes U (2012). Spectrum of pore types and networks in mudrocks and a descriptive classification for matrix-related mudrock pores. AAPG

Bulletin, 96(6): 1071-1098.
https://doi.org/10.1306/08171111061

McCreesh CA, Ehrlich R, and Crabtree SJ (1991). Petrography and reservoir physics ii: relating thin section porosity to capillary pressure, the association between pore types and throat size (1). AAPG Bulletin, 75(10): 1563-1578.

Morad S, Ketzer JRM, and De Ros LF (2000). Spatial and temporal distribution of diagenetic alterations in siliciclastic rocks: Implications for mass transfer in sedimentary basins. Sedimentology, 47(s1): 95-120.
https://doi.org/10.1046/j.1365-3091.2000.00007.x

Nelson R (2001). Geologic analysis of naturally fractured reservoirs. Elsevier, New York, USA.

Nelson RA and Handin J (1977). Experimental study of fracture permeability in porous rock. AAPG Bulletin, 61(2): 227-236.

Petrocelli JV (2003). Hierarchical multiple regression in counseling research: Common problems and possible remedies. Measurement and Evaluation in Counseling and Development, 36(1): 9-22.

Pettijohn FJ, Potter PE, and Siever R (1973). Sand and Sandstone. Springer, Heidelberg, Germany.
https://doi.org/10.1007/978-1-4615-9974-6

Rahman AHA, Menier D, and Mansor MY (2014). Sequence stratigraphic modelling and reservoir architecture of the shallow marine successions of Baram field, West Baram Delta, offshore Sarawak, East Malaysia. Marine and Petroleum Geology, 58: 687-703.
https://doi.org/10.1016/j.marpetgeo.2014.03.010

Rijks EJH (1981). Baram delta geology and hydrocarbon occurrence. Geological Society of Malaysia Bulletin, 14: 1-18.

Ringrose P and Bentley M (2015). Reservoir model types. In: Ringrose P and Bentley M (Eds.), Reservoir model design: 173-231. Springer, Dordrecht, Netherlands.
https://doi.org/10.1007/978-94-007-5497-3_6

Savoy LE, Stevenson RK, and Mountjoy EW (2000). Provenance of upper devonian-lower carboniferous miogeoclinal strata, southeastern Canadian Cordillera: Link between tectonics and sedimentation. Journal of Sedimentary Research, 70(1): 181-193.
https://doi.org/10.1306/2DC40909-0E47-11D7-8643000102C1865D

Surek MA (2013). Cluster analysis of the balakhany viii reservoir unit with spectral gamma ray logs azeri-chirag-gunashli field, offshore Azerbaijan. M.Sc. Thesis, University of Houston, Houston, Texas, USA.

Tan DNK, Rahman AHB, Anuar A, Bait B, and Tho CK (1999). West Baram Delta. In: Leong KM (Ed.), The petroleum geology and resources of Malaysia: 293-341. Malaysian National Petroleum Corporation, Kuala Lumpur, Malaysia.

Tiab D and Donaldson EC (2015). Petrophysics: Theory and practice of measuring reservoir rock and fluid transport properties. Gulf Professional Publishing, Houston, Texas, USA. **PMCid:PMC4803137**

Udden JA (1914). Mechanical composition of clastic sediments. Bulletin of the Geological Society of America, 25(1): 655-744.
https://doi.org/10.1130/GSAB-25-655

Weijermars R and van Harmelen A (2017). Advancement of sweep zones in waterflooding: Conceptual insight based on flow visualizations of oil-withdrawal contours and waterflood time-of-flight contours using complex potentials. Journal of Petroleum Exploration and Production Technology, 7(3): 785-812.
https://doi.org/10.1007/s13202-016-0294-y

Welton JE (1984). SEM petrology atlas. The American Association of Petroleum Geologists Tulsa, Oklahoma, USA.

Wentworth CK (1922). A scale of grade and class terms for clastic sediments. The Journal of Geology, 30(5): 377-392.
https://doi.org/10.1086/622910